

Calibration of GEO 600 for the S1 science run

**M Hewitson¹, H Grote², G Heinzl², K A Strain¹, H Ward¹
and U Weiland³**

¹ Department of Physics & Astronomy, University of Glasgow, Glasgow G12 8QQ, UK

² Max-Planck-Institut für Gravitationsphysik, Albert-Einstein-Institut, Außenstelle Hannover, Callinstr. 38, 30167 Hannover, Germany

³ Institut für Atom- und Molekülphysik, Universität Hannover, Callinstr. 38, 30167 Hannover, Germany

E-mail: hewitson@astro.gla.ac.uk

Received 23 April 2003

Published 18 August 2003

Online at stacks.iop.org/CQG/20/S885

Abstract

In 2002, the interferometric gravitational wave detector GEO 600 took part in a coincident science run (S1) with other detectors world-wide. When completed, GEO will employ a dual-recycling scheme which will allow its peak sensitivity to be tuned over a range of frequencies in the detection band. Still in the commissioning phase, GEO was operated as a power-recycled Michelson for the duration of S1. The accurate calibration of the sensitivity of GEO to gravitational waves is a critical step in preparing GEO data for exchange with other detectors forming a world-wide detector network. An online calibration scheme has been developed to perform real-time calibration of the power-recycled GEO detector. This scheme will later be extended to cover the more complex case of the dual-recycled interferometer in which multiple output signals will need to be combined to optimally recover a calibrated strain channel. This report presents an outline of the calibration scheme that was used during S1. Also presented are results of detector characterization work that arises naturally from the calibration work.

PACS numbers: 04.80.Nn, 95.55.Ym, 95.75.Kk

(Some figures in this article are in colour only in the electronic version)

1. Introduction

GEO 600 is a gravitational wave observatory situated near Hannover, Germany. The detector is currently undergoing the final stages of hardware installation and will soon enter a phase of optimization followed by continuous operation. When fully commissioned GEO should be one of the most sensitive displacement measuring instruments in the world, capable of

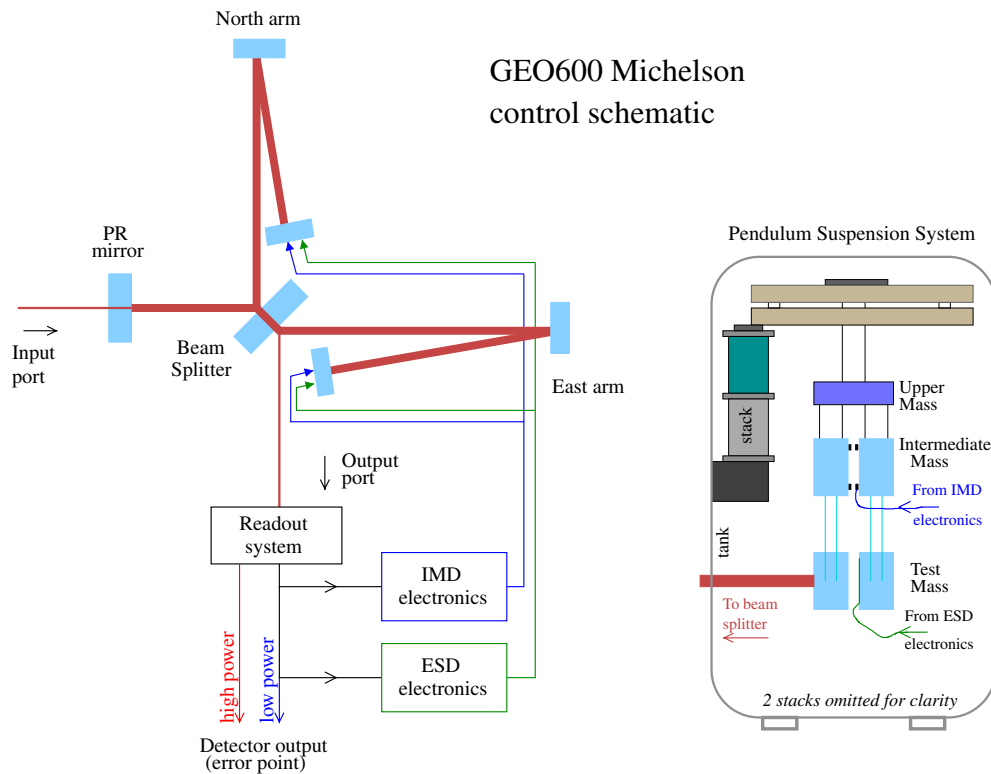


Figure 1. A schematic of the Michelson lock for GEO 600. The electrostatic drive (ESD) applies high-frequency correction forces to the mirror. The intermediate mass drive (IMD) applies low-frequency corrections to the intermediate mass. In reality the arms are folded in a vertical plane, and are shown here in the horizontal plane for convenience.

measuring differential displacements of the two 1200 m arms of the order $10^{-19} \text{ m}/\sqrt{\text{Hz}}$ in the frequency band 50 Hz to a few kHz.

The optical layout of GEO is based on the standard Michelson interferometer but differs by the addition of two mirrors [4]: the power recycling (PR) mirror, which will increase the circulating light power in the detector helping to lower shot-noise level, and the signal recycling (SR) mirror which forms a resonant cavity with the power-recycled Michelson that enhances signals in a chosen frequency band. Figure 1 shows a simplified schematic of the optical layout. For the S1 science run, GEO was operated as a power-recycled Michelson as the signal recycling mirror was yet to be installed.

One of the main science goals of S1—which took place in the summer of 2002 and was attended by GEO, the three LIGO detectors [1], the ALLEGRO bar detector and, for some of the time, by TAMA [2]—was to set upper limits to the gravitational wave emission from a variety of astronomical sources. These sources are usually split into four broad source areas: signals arising from the inspiralling of compact objects (neutron stars, black holes), periodic signals (from pulsars for example), signals from the stochastic gravitational wave background, and short duration burst-type signals. In order to interpret the detector output signals in an astrophysically meaningful way, it is necessary to perform an accurate calibration.

In the power-recycled configuration of GEO, a single output channel contains all the gravitational wave information and so this calibration can be performed after recognition of

candidate events. In the dual-recycled interferometer, the gravitational wave information is contained in multiple channels and it is the calibration process that will combine these to produce an optimal calibrated strain channel. This makes it necessary that calibration is done before any astrophysical searches are performed. Within GEO, the decision was made to concentrate on producing calibrated data streams that can be presented to the individual search pipelines.

2. An overview of the Michelson locking scheme

The control system of GEO 600 comprises many feedback paths that aim to keep the detector aligned and locked to the correct operating point. The calibration of the power-recycled Michelson relies only on the determination of the servo loop that controls the Michelson differential arm length lock. The Michelson control servo uses a split feedback servo that senses, and minimizes, deviations from the dark-fringe operating point (see figure 1). Large dynamic range low-frequency feedback signals are applied with coils and magnets to an intermediate mass drive (IMD) from which the main (test mass) mirror is suspended, whereas small amplitude high-frequency feedback signals are applied directly to the test mass via an electrostatic drive (ESD). The noise performance of the detector during S1 was such that the error-point signal of the Michelson servo could be recorded with a high signal-to-noise ratio across the entire detection band (50 Hz to 6 kHz). The error signal, along with the details of the servo loop, contains all the information necessary to calibrate the detector output. Although the calibration of the feedback actuator was observed to remain constant, at least over the duration of the science run, the presence of tidal drifts, temperature fluctuations and seismic disturbances can all cause the sensitivity of the detector to vary in a time-dependent way. In order to compensate for any of these drifts, the calibration of the detector must be updated sufficiently often.

During the S1 science run, two photodiodes were used to sense the output light of the interferometer: a low-power quadrant photodiode used in the Michelson servo-loop and the auto-alignment system, and a high-power photodiode to give a high signal-to-noise ratio measure of the output light. The differential mirror displacement and hence the detected strain signal were determined from the high-power photodiode signal.

3. A summary of the calibration procedure employed in S1

The length change, ΔL , of each arm, induced when an optimally oriented gravitational wave of amplitude $h(t)$ passes through GEO can be expressed as

$$h(t) = 2 \frac{\Delta L(t)}{L}, \quad (1)$$

where L is 1200 m for GEO. To calibrate GEO we must determine the differential displacement, ΔL , from the recorded detector output. To do this we must determine the frequency-dependent, time-varying, detector (optical) gain. In the power-recycled GEO, the frequency response of the optical gain is flat but the detector output is modified in a frequency-dependent way by the presence of the Michelson control loop; in the case of the dual-recycled GEO, the detector gain will have a frequency-dependent response arising from the optical cavity formed between the SR mirror and the Michelson interferometer.

It is necessary to consider the calibration in two frequency regimes: a high-frequency regime where the Michelson control servo has no loop gain (>200 Hz) and a low-frequency regime where the loop gain of the servo is significant (the unity gain point of the servo was

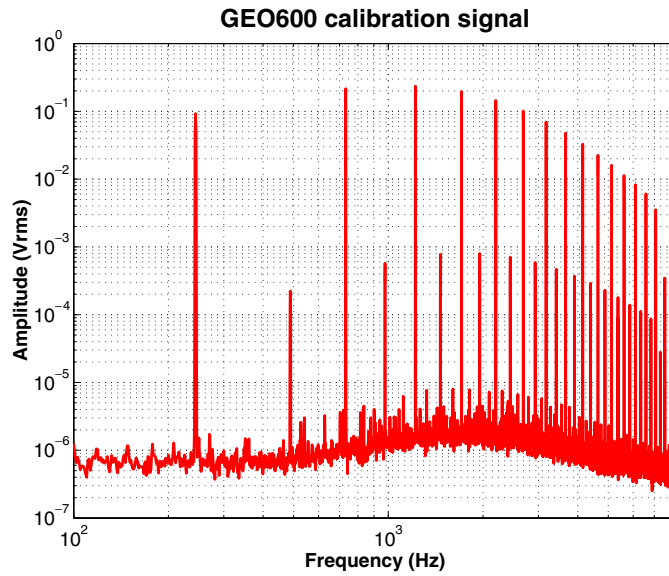


Figure 2. Spectrum of the calibration signal applied to the ESD.

around 100 Hz in S1). At frequencies well above the unity gain point of the Michelson servo the optical gain can be determined simply by displacing the end mirrors by a known amount and then observing the signal in the detector output. For the low-frequency calibration, the loop gain of the Michelson servo must be continually determined. The following text outlines the calibration method that was used. A more detailed description can be found in [5]. Throughout S1, a known mirror motion was induced continuously at particular frequencies by injecting a calibration signal into the electrostatic drive feedback path. The signal was composed of a set of spectral peaks derived by differentiating the signal from a square-wave oscillator such that the displacement induced by the first four odd harmonics was approximately uniform. The oscillator was locked to a GPS frequency standard. Since the DAQ sample clock was also locked to a GPS frequency standard, we were able to ensure that all the power from a particular spectral peak was confined to one spectral bin in the analysis. Figure 2 shows a spectrum of the recorded calibration signal that was injected into the ESD. Figure 3 shows the calibration peaks as they appear in a snap-shot spectrum of the Michelson servo error-point.

The optical gain of the detector (denoted H_1 in figure 4) was estimated once per second as

$$H_{1f} = \frac{|y_f|}{|x_f|H_{5f}}, \quad (2)$$

where y_f is the calibration peak amplitude measured in the error-point spectrum, x_f is the calibration peak amplitude applied to the electrostatic drives and H_{5f} is the electrostatic drive response which has a $1/f^2$ response above the pendulum resonance [3] (as seen in figure 4). The subscript f denotes evaluation at a particular frequency. Equation (2) was evaluated at frequencies corresponding to the first three harmonics (732, 1220 and 1708 Hz). These three independent estimates of the optical gain were combined (each weighted by their individual signal-to-noise ratios), to give a single value for the optical gain once per second. Having determined the calibration factor for high frequencies (the optical gain) we then need to determine the low-frequency (<200 Hz) calibration factor as a function of frequency. This was done using a model of the Michelson control servo. The model used is shown in figure 4,

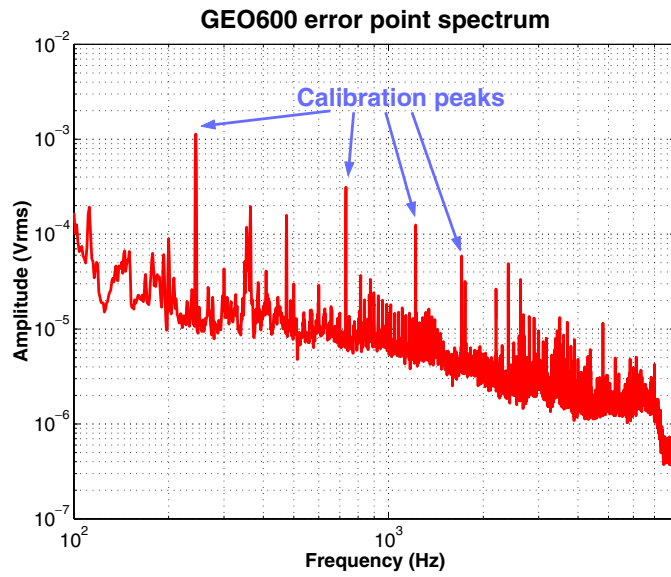


Figure 3. An error-point spectrum derived from the high-power photodiode output of GEO taken by averaging ten 1 s data segments. The effect of the $1/f^2$ frequency response [3] of the ESD actuator on the calibration peaks can be seen clearly.

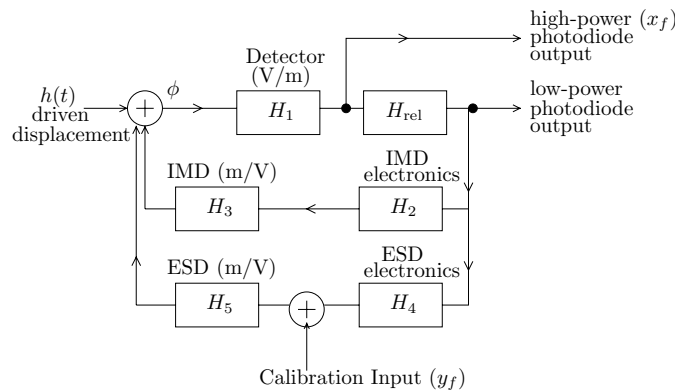


Figure 4. A model of the Michelson lock of GEO 600.

in which the optical gain is denoted by H_1 , the relative gain between the two photodiodes by H_{rel} , and the two feedback paths by H_2H_3 and H_4H_5 . Determination of all the elements of this model allows the loop gain to be calculated at all frequencies where the model is valid (10 Hz to ~ 6 kHz).

In order to perform the calibration of the detector in real time, the calibration function (the inverse of the servo transfer function from mirror displacement to volts at the error-point) was implemented in the time-domain using infinite impulse response (IIR) filters. A time domain function was derived using IIR filters, F_{rel}, F_1, \dots, F_5 , in place of the frequency domain transfer functions, H_{rel}, H_1, \dots, H_5 , shown in figure 4. Thus, for a recorded detector output, $v(t)$, we can determine the time-varying mirror displacement, $\Delta L(t)$, by applying these filters

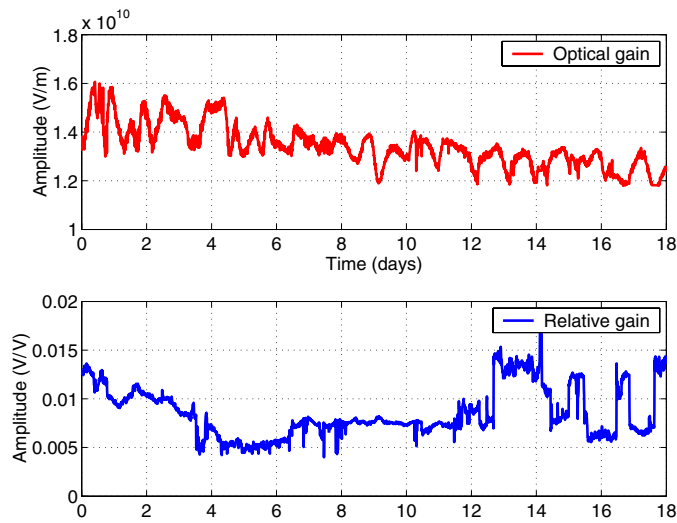


Figure 5. The time evolution of the optical gain and relative gain between the two photodiodes derived from the calibration process. The data shown are sampled every 10 min and cover the whole S1 run.

in the appropriate combination. The following equation shows the implementation of this calibration equation:

$$\Delta L(t) = v(t) * \{F'_1 + F_{\text{rel}} * (F_2 * F_3 + F_4 * F_5)\}, \quad (3)$$

where $*$ denotes convolution and F'_1 is the IIR filter matching the inverse of H_1 . The recovered displacement signal can then be converted to a strain signal using equation (1).

Using the measured optical gain and the filters developed for the electronics and feedback actuators of the servo, the calibration equation was applied continuously throughout S1 providing an online calibrated strain channel that was recorded to disk along with all the other detector and environmental channels.

4. Results and detector characterization from S1

Having the calibration signal injected over long periods of time provides a good way of investigating long-term drifts and fluctuations in the detector's performance. In S1, the detector remained locked for around 98% of the 18 days of the run. Figure 5 shows the time evolution of both the optical and relative gains for the entire S1 run.

For the optical gain, we can see variations of around 7% on time scales of a day as well as a general drop of around 20% in the optical gain over the entire run. The daily variations correlate well with the temperature in the central station. Figure 6 shows a magnified portion of the optical gain overlaid with the temperature recorded on the laser bench. These variations are a small effect as we can see when we look at a spectrum of the optical gain and compare it to the daily variations of the longitudinal feedback for example.

Figure 7 shows spectra of the optical gain and the Michelson differential longitudinal feedback for periods of a few days down to periods of an hour or so. We can clearly see a diurnal variation in the differential feedback signal but the optical gain shows no significant peak. In addition we clearly see the lunar tides in the differential feedback but again the

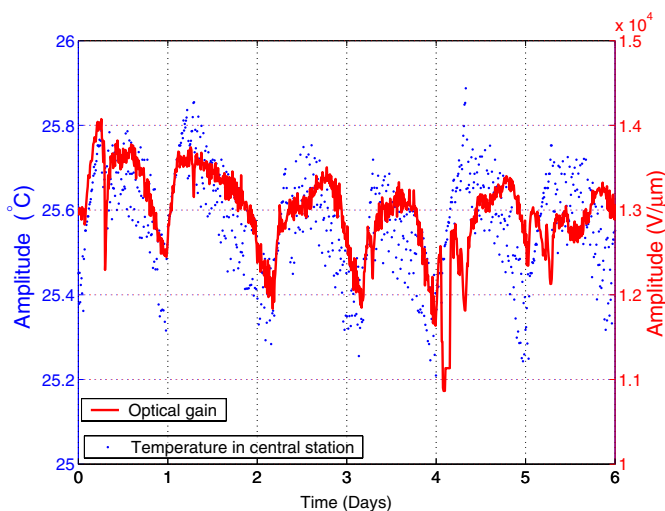


Figure 6. The optical gain overlaid with the temperature as measured on the laser bench in the central station. Both time series are sampled once every 10 min.

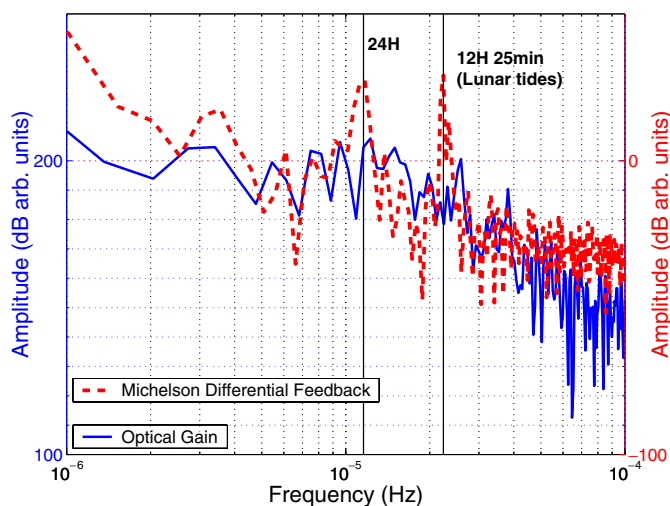


Figure 7. Low-frequency spectra of the optical gain and the Michelson differential feedback signals. Each spectra uses datasets sampled once per minute. No averaging is performed in order to present the highest resolution possible.

optical gain shows no significant effect. The absence of the moon tide peak in the optical gain demonstrates that any residual coupling of longitudinal feedback into alignment fluctuations is sufficiently small or is adequately compensated by the auto-alignment system.

Using a different resolution of spectrum we can see another prominent variation in the optical gain: ~ 19.5 min. This is thought to be a temperature-related variation coming from the air conditioning unit in the central station. Figure 8 shows this variation as it appears in a spectrum of the optical gain.

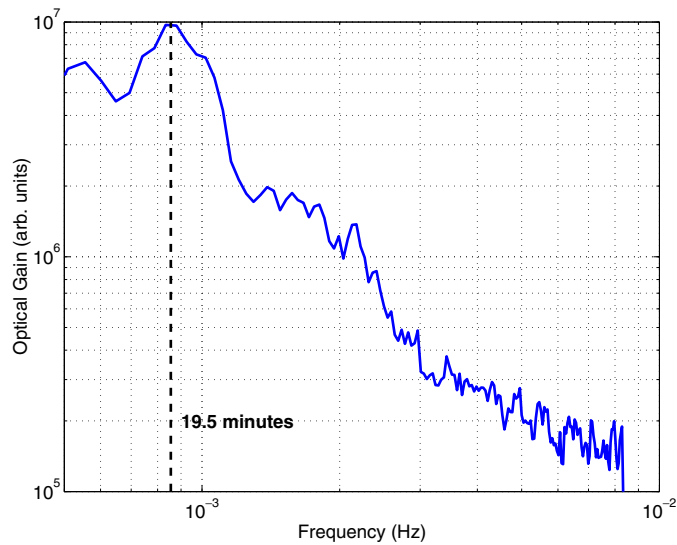


Figure 8. A spectrum of the optical gain showing a 19.5 min peak believed to arise from the airconditioning switching on and off in the central station.

The relative gain is somewhat more erratic towards the end of the run. At times we see large excursions (up to a factor of 2) occurring over short time scales. The reasons for these sharp changes are not known at this time but they possibly come from changes in the output beam position. Saturation of some of the beam position sensors may have caused the output beam position to drift. The quadrant photodiode is particularly sensitive to changes of this kind since the incident spot is quite large (a few mm) at this point compared to the 10 mm diameter of the photodiode. It is possible that if the beam position moved slightly it may have been clipped somewhere on the output bench. The output beam is focused before it is allowed to fall on the high-power photodiode making this signal more insensitive to fluctuations in beam position.

Over the first 4 days of the run we can see a steady drop in the relative gain. One possible explanation for this decay is that it comes from slight position changes and settling of the components on the output bench. The output bench was set up prior to the run and then not adjusted again during the run.

5. Summary

The S1 science run proved to be an excellent opportunity to test the online calibration scheme for GEO. The ability to track and study the stability of the calibration (and hence the detector) over long time scales was invaluable. Although a few areas were found where improvements can be made, in general the scheme proved a successful first experiment and produced a continuous real time $h(t)$ for the entire duration of the S1 science run. A study of the errors in the procedure (discussed more thoroughly in [5]) leads to a calibration accuracy of around 4% at high frequencies (>200 Hz) and about 6% for frequencies between about 50 Hz and 200 Hz.

Further calibration work will need to focus on the problems and deficiencies highlighted in this first experiment. Additionally, the introduction of the signal-recycling mirror into

GEO will require a more sophisticated calibration scheme since the frequency response of the signal-recycling cavity may vary over time. Furthermore the gravitational wave signal will no longer be contained in a single demodulation quadrature of the output photodiode, resulting in the need to calibrate and combine multiple output signals in order to obtain a single calibrated strain channel.

References

- [1] Sigg D 2001 Commissioning of the LIGO detectors *Class. Quantum Grav.* **19** 2002
- [2] Ando M 2001 Japanese large-scale interferometers *Class. Quantum Grav.* **19** 2002
- [3] Plissi M V, Torrie C I, Husman M E, Robertson N A, Strain K A, Ward H, Lück H and Hough J 2000 GEO 600 triple pendulum suspension system: seismic isolation and control *Rev. Sci. Instrum.* **71** 2539–45
- [4] Heinzl G, Freise A, Grote H, Strain K A, Hough J and Danzmann K 2002 Dual Recycling for GEO 600 *Class. Quantum Grav.* **19** 1547
- [5] Hewitson M *et al* 2003 Calibration of the power-recycled GEO 600 *Rev. Sci. Instrum.* at press